# Nanopaleomagnetism of Meteoritic Fe-Ni: the Potential for Time-Resolved Remanence Records within the Cloudy Zone

**Richard J Harrison**[1], James F J Bryson[1], Takeshi Kasama[2], Nathan S Church[1], Julia Herrero Albillos[3], Florian Kronast[4], Massimo Ghidini[1], Simon A T Redfern[1], Gerrit van der Laan[5], Tolek Tyliszczak[6]

[1] University of Cambridge, U.K. (rjh40@cam.ac.uk) [2] Technical University of Denmark [3] Centro Universitario de la Defensa + Universidad de Zaragoza, Spain [4] BESSYII Synchrotron Source, Germany [5] Diamond Light Source, U.K. [6] Advanced Light Source, U.S.

## Summary/Conclusions

1. Paleomagnetic signals recorded by meteorites provide compelling evidence that the liquid cores of differentiated asteroids generated magnetic dynamo fields.
2. Magnetic nanostructures unique to meteoritic Fe-Ni metal are capable of carrying a time-resolved record of asteroid dynamo activity.
3. Dramatic changes in magnetic properties are associated with the transition from kamacite – tetrataenite rim – cloudy zone – plessite, typical of Fe-Ni intergrowths.
4. The cloudy zone (CZ) forms via a process of spinodal decomposition during slow cooling at temperatures below ~ 400°C. It is made up of nanoscale islands of tetrataenite (FeNi) coherently intergrown with a hitherto unobserved soft magnetic phase ($Fe_3Ni$).
5. Each tetrataenite island is uniformly magnetised along one of six <100> crystallographic directions. The populations of these six states can be measured using X-ray photo-emmision electron microscopy to provide a measure of natural remanence on a submicron length scale.
6. Analysis of the Tazewell IIICD iron meteorite reveals that all three easy axes are equally populated in the course to intermediate CZ, suggesting that CZ formation in those regions was not influenced by internal interaction fields. The fine CZ shows strong preference for one easy axis, suggesting CZ formation in that region was strongly influenced by interaction with the neighbouring plessite.
7. Course and intermediate CZs within the Imilac and Esquel pallasites show an unequal distribution of tetrataenite magnetisation directions, consistent with their formation in an external field > 1.5-3.5 $\mu$T.
8. Under favourable circumstances, the techniques developed here could be used to determine the time-dependence of an asteroid dynamo field, with variations in the net remanence vector at the sub-micron scale reflecting variations in the intensity and relative direction of magnetic fields present during cooling.

## Transmission Electron Microscopy of the Tazewell IIICD Cloudy Zone

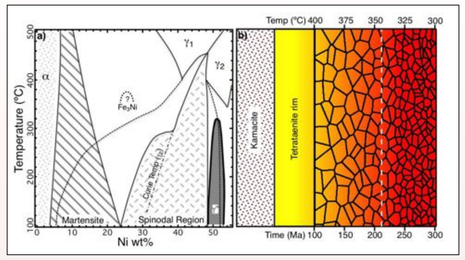


**Fig. 1.** (a) Low-temperature portion of the Fe-Ni phase diagram. (b) Schematic diagram of the sequence kamacite – tetrataenite – CZ that forms in meteoritic Fe-Ni metal during slow cooling. Ni content (yellow: 50%Ni, red: 25%Ni) and tetrataenite island size decrease throughout the CZ. Temperatures and times of CZ formation in metal formed 10 km from the surface of a 200 km radius parent body are indicated. The dashed white line indicates the time and temperature of core solidification for such a body.

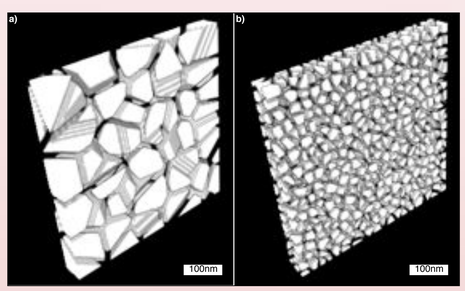


**Fig. 3.** Three-dimensional representations of the CZ used to simulate the holography results. The dimensions of the islands and matrix match those observed experimentally.

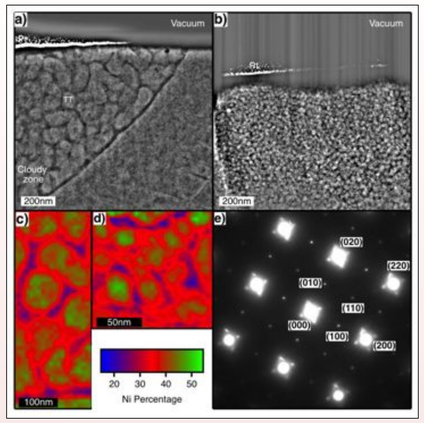


**Fig. 2.** STEM images of (a) course and (b) fine regions of the CZ (bright = tetrataenite, dark = matrix). (c, d) Composition maps of the intermediate CZ with islands 50%Ni:50%Fe and matrix 25%Ni:75%Fe. (e) Diffraction pattern representative of both the coarse and fine CZ.

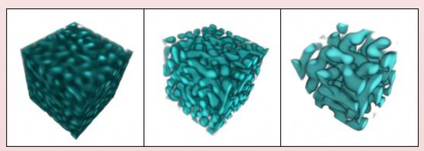

**Fig. 4.** Computer simulations of spinodal decomposition in an isotropic medium, showing progressive development and coarsening of the island/matrix nanostructure.

## Electron Holography Remanence Hysteresis

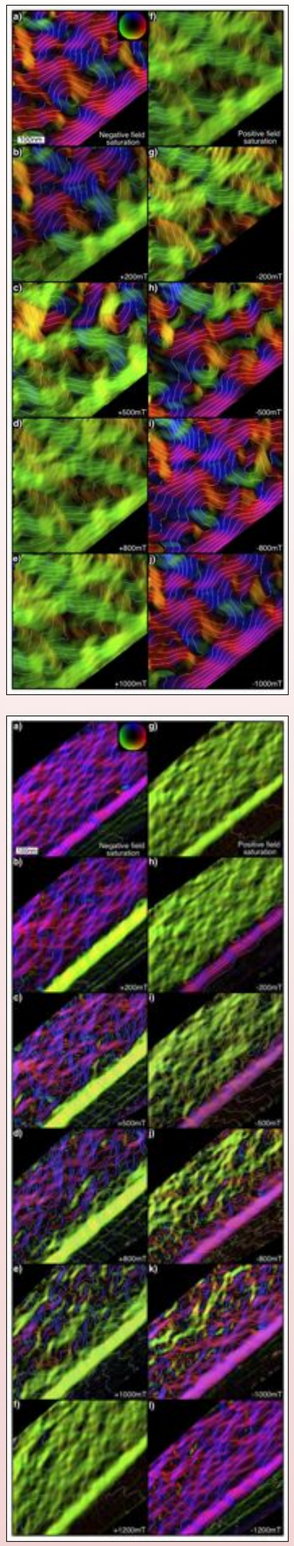


## Electron Holography Interpretation

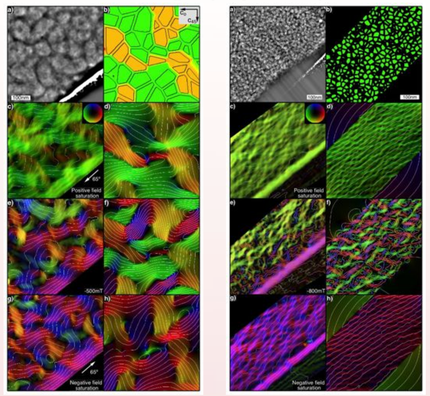

**Fig. 5.** Experimental (left) and simulated (right) holography images of the coarse and fine CZ. The CZ corresponds to a natural nanocomposite of magnetically hard tetrataenite islands and a magnetically soft matrix composed of atomically ordered $Fe_3Ni$ with the L12 structure. The matrix magnetisation is similar in strength to that of tetrataenite in the coarse CZ and decreases in intensity throughout the CZ. Tetrataenite islands (up to the maximum ~100 nm diameter observed) display uniformly magnetised single domain states at remanence. The switching field of the coarse CZ is significantly lower than that of the fine CZ.

## Micromagnetic Simulation

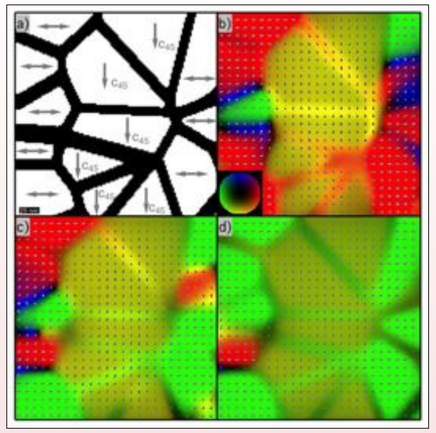

**Fig. 6.** Micromagnetic simulations that mimic the experimental sample/field geometry. a) Easy axis orientations. b) Remanent state after application of a saturating in-plane field to the right. c) Result after 0.36 T in-plane field to the left. d) Result after 1 T in-plane field to the left. Switching occurs via the nucleation of domain walls in the matrix followed by their propagation through individual islands. The coercivity of the coarse CZ is lowered due to exchange coupling with the soft magnetic matrix, which aids the nucleation and penetration of domain walls into the tetrataenite islands. This effect explains the systematic variation in coercivity with length scale of the nanostructure throughout the CZ.

European Research Council
Established by the European Commission
NERC SCIENCE OF THE ENVIRONMENT
The Leverhulme Trust
UNIVERSITY OF CAMBRIDGE

## X-ray Photo-Emission Electron Microscopy (X-PEEM)

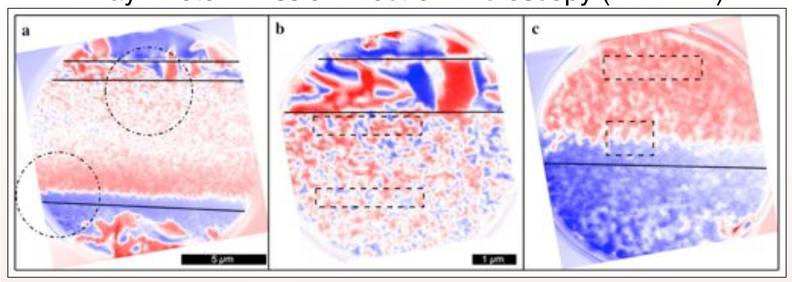


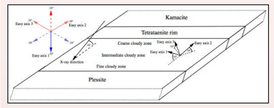


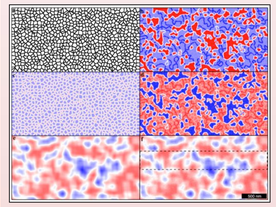

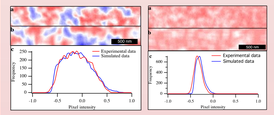

**Fig. 7** (above) X-PEEM images of a polished (111) surface of the Tazewell, after application of a 1 T out-of-plane field. Blue and red signals indicate components of magnetisation that are parallel and antiparallel to the X-ray beam direction, respectively. (a) 15 $\mu$m field-of-view showing magnetic domain states across the sequence (top to bottom) kamacite, tetrataenite rim, coarse-intermediate-fine CZ and plessite. (b) 5 $\mu$m field-of-view of kamacite, tetrataenite rim and coarse CZ. (c) 5 $\mu$m field-of-view of the fine CZ. The boundary between red and blue is an irregular domain wall that failed to penetrate into the finest CZ in a 1 T field.

**Fig. 8** (left). (a) 2D cells used to simulate the island/matrix nanostructure. In-plane (b) and out-of-plane (c) component of magnetisation assigned via random choice of three easy axes. Note constant out-of-plane component due to application of 1 T field. (d) Projection of magnetisation along X-ray beam direction. Simulated X-PEEM signal after applying (e) instrumental resolution function and (f) noise.

**Fig. 9** (left) Comparison of observed (upper) and simulated (lower) images for the course and fine CZ. Quantitative comparison of observed and simulated X-PEEM intensities, demonstrating equal populations of all three easy axes in the coarse CZ and strong alignment along one easy axis in the fine CZ.

## X-PEEM of Pallasites

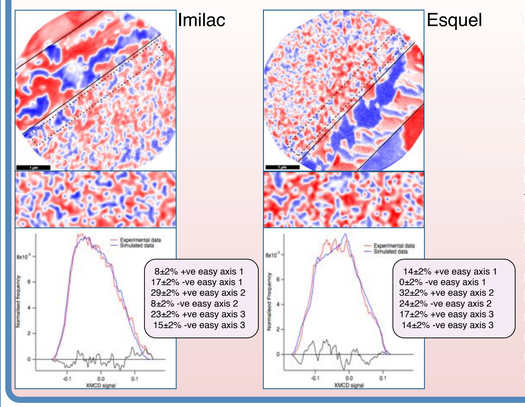


**Fig. 10**. 5 $\mu$m field-of-view X-PEEM images of the coarse CZ within the Imilac (left) and Esquel (right) pallasites. Samples were not exposed to a magnetic field prior to measurement. Quantitative analysis allows, therefore, all six of the possible tetrataenite island magnetisation states (and therefore the NRM vector) to be determined for individual sub-micron regions of interest. Due to the high intrinsic anisotropy of tetrataenite, the surface magnetisation is representative of the bulk magnetisation. Self consistent results are obtained from several regions, all showing that there is an unequal population of the six states (i.e. the CZ carries an NRM).

## Chemical Transformation Remanent Magnetisation (CTRM)

**Fig. 11.** The CZ can be considered as massively multi-domain, with the domain size of the order of the island size. To obtain a lower limit of the paleofield we assume that CTRM is blocked when the islands reached their present volume. Each island can adopt one of six magnetisation states with proportions determined by their thermodynamic probability (assuming chemical equilibrium w.r.t. to the applied field), e.g.:

$$\frac{\langle n_{+x}\rangle}{N} = \frac{e^{\frac{-MB_x}{k_BT}}}{e^{\frac{-MB_x}{k_BT}} + e^{\frac{MB_x}{k_BT}} + e^{\frac{-MB_y}{k_BT}} + e^{\frac{MB_y}{k_BT}} + e^{\frac{-MB_z}{k_BT}} + e^{\frac{MB_z}{k_BT}}}$$

This provides a lower limit of the paleofield of > 3.5 $\mu$T and > 1.5 $\mu$T for the Imilac and Esquel pallasites, respectively. The required fields are greater (~10-100 $\mu$T) if CTRM blocks before the islands reach their final volume.